Predicting Rib Fracture Risk With Whole-Body Finite Element Models: Development and Preliminary Evaluation of aProbabilistic Analytical Framework

Jason L. Forman, Richard W. Kent
University of Virginia Center for Applied Biomechanics

Krystoffer Mroz, Bengt Pipkorn, Ola Bostrom
Autoliv Research

Maria Segui-Gomez
European Center for Injury Prevention

ABSTRACT – This study sought to develop a strain-based probabilistic method to predict rib fracture risk with whole-body finite element (FE) models, and to describe a method to combine the results with collision exposure information to predict injury risk and potential intervention effectiveness in the field. An age-adjusted ultimate strain distribution was used to estimate local rib fracture probabilities within an FE model. These local probabilities were combined to predict injury risk and severity within the whole ribcage. The ultimate strain distribution was developed from a literature dataset of 133 tests. Frontal collision simulations were performed with the THUMS (Total HUman Model for Safety) model with four levels of delta-V and two restraints: a standard 3-point belt and a progressive 3.5-7 kN force-limited, pretensioned (FL+PT) belt. The results of three simulations (29 km/h standard, 48 km/h standard, and 48 km/h FL+PT) were compared to matched cadaver sled tests. The numbers of fractures predicted for the comparison cases were consistent with those observed experimentally. Combining these results with field exposure informantion (ΔV, NASS-CDS 1992-2002) suggests a 8.9% probability of incurring AIS3+ rib fractures for a 60 year-old restrained by a standard belt in a tow-away frontal collision with this restraint, vehicle, and occupant configuration, compared to 4.6% for the FL+PT belt. This is the first study to describe a probabilistic framework to predict rib fracture risk based on strains observed in human-body FE models. Using this analytical framework, future efforts may incorporate additional subject or collision factors for multi-variable probabilistic injury prediction.

INTRODUCTION

The thorax is one of the most commonly injured body regions in automobile collisions. The thorax accounts for approximately 30% of injures to belted drivers over the age 34 fatally injured in frontal collisions (Kent et al., 2005a). The most common type of skeletal thoracic injuries sustained by restrained occupants in frontal collisions are rib fractures (Pattimore et al., 1992). Rib fractures are generally associated with an increased risk of mortality, especially for the elderly (Kent et al., 2008). Among persons over the age of 60 who die of chest injuries in automobile collisions, approximately 40% experience rib fractures as the most severe chest injury (Kent et al., 2005b).

CORRESPONDING AUTHOR:
Jason L. Forman, PhD, Center for Applied Biomechanics, University of Virginia, 4040 Lewis & Clark Dr., Charlottesville, VA, USA; Email: jlf3m@virginia.edu

Protecting automobile occupants against chest injury requires an ability to predict the occurrence of rib fractures during a simulated collision or crash test. There exist several different methods to predict the occurrence of rib fractures using finite element (FE) computer models of the body. These methods may be classified into two categories: deterministic and probabilistic. Deterministic models are designed to predict an exact occurrence (or number) of fractures based on a single set of model (occupant) characteristics. This includes element-elimination or element softening methods where elements are removed from the rib models (representing fracture) or allowed to yield freely when the strain in the elements exceed a specified threshold (e.g., Kent et al., 2005b). Deterministic methods are limited, however, in that they are designed to predict fracture in a binary fashion (yes or no) based on a specific set of occupant characteristics. As a result, deterministic methods are limited in their ability to predict injury occurrence in a population with varying physical characteristics.

In contrast, probabilistic methods attempt to predict the probability of injury in a given scenario, affected by variations in occupant or collision characteristics. Empirical probabilistic methods are commonly used for predicting injury risk based on measurements made by physical dummies during crash tests (e.g., Laituri et al., 2005). Such models are usually developed in a "top-down" approach by relating injury occurrence (often in a cadaver model) to dummy measures in matched collision conditions. Because of the level of modeling detail possible, it may be possible to incorporate probabilistic analyses into FE model injury prediction in a more "bottom-up", or causal, manner by incorporating variations in subject or collision characteristics into the FE simulation strategy. This may represent an improvement over empirical strategies by allowing injury prediction based on known variations in anthropometry, skeletal mechanics, pathology, etc.

FE-based probabilistic methods have been explored on a limited basis for the prediction of injury in some body regions (e.g., cervical spine; Francis et al., 2005; Thacker et al., 1997). Such methods have not gained widespread adoption, however, in part due to a real or perceived computational cost required to perform such analyses. When a "bottom-up" probabilistic analysis seeks to include a distributed variable that affects the output of the FE model (e.g., a bone material model or a characteristic of the model geometry), multiple distinct simulations must be performed with values of the variable of interest spanning the distribution range. If several such variables are studied, the number of simulations required to study interaction effects multiplies accordingly. Therefore, the computational investment required may turn prohibitive if multiple model-affecting variables are studied.

The overall goal of this study was to explore a framework, or strategy, for probabilistic injury prediction for use with human body FE models, designed within the practical confines of computational time investment. The first goal was to develop an analysis strategy for the prediction of rib fracture risk incorporating known variations in rib cortical bone ultimate strain. The ultimate strain is the strain threshold at which material failure (fracture) is expected to occur. The ultimate strain of rib cortical bone has been shown to vary in the population (Kemper et al., 2005; Kemper et al., 2007), including a decreasing relationship with age (Carter and Spengler, 1978). If it is assumed that a relatively small number of rib fractures do not affect either the overall stiffness of the ribcage (Kent et al., 2004; Duma et al., 2006; Kemper et al., 2011), or the strain occurring in other ribs, then the definition of rib cortical bone ultimate strain will not substantially affect the output of a model of the ribcage. As a result, it may be possible to use probabilistic methods to estimate the risk of rib fracture based on a distribution of ultimate strain values without the need to perform large numbers of simulations. This study sought to develop a probabilistic method to predict rib fracture risk from FE simulations, based on variations in rib cortical bone ultimate strain within a prescribed distribution based on information in the literature (Kemper et al., 2005; Kemper et al., 2007). This study also explored variations in rib fracture risk with age based on a previously-described relationship between rib ultimate strain and age (Carter and Spengler, 1978).

The second goal of this study was to describe a simulation and analysis strategy incorporating variations in FE model input parameters (in this case, collision ΔV), and fitting the risk outputs from a discrete sample of simulations to a parametric risk response surface (or curve). Such methods are commonly used in other engineering disciplines studying probabilistic failure mechanics (e.g., Rahman, 2001), and can substantially reduce the number of simulations required to describe failure probability within a variable distribution space. The final goal of this study was to combine an age-dependent risk-response curve relating ΔV to injury risk with a real-world, field distribution of collision ΔVs to illustrate how this type of causal, FE based probabilistic analysis may be applied to predict injury risk in the field.

METHODS

This study consisted of two major goals: 1) Develop a causal probabilistic method to predict rib fracture risk based on strain outputs from human body FE models (and explore preliminary evaluation and validation); and 2) Describe a method to generate risk response curves from simulations performed across a range of input conditions, and to combine those results with exposure information to predict a risk of injury in the field. The overall strategies for those two goals are shown in the flowcharts of Figure 1a and 1b (respectively).

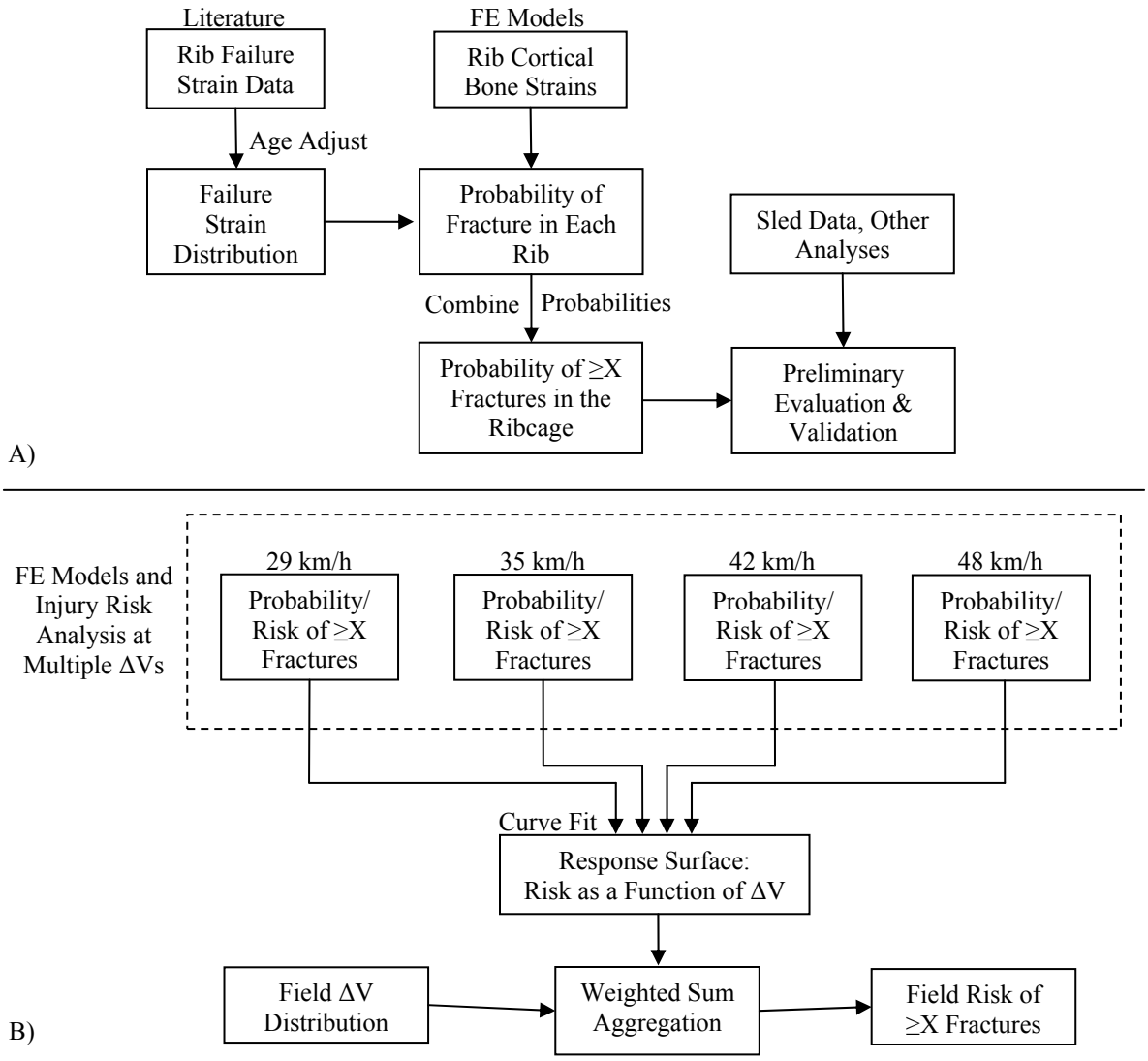

Figure 1: Flow charts illustrating the methods developed in this study for predicting rib fracture risk based on strain outputs from human body FE models. A) Outline of the method for predicting the risk of incurring greater than or equal to an arbitrary number (≥X) fractures based on the strain output from a simulated collision and based on age-adjusted variations in rib cortical bone ultimate strain in a sample population. B) Outline of the method for predicting an exposure-weighted risk of ≥X fractures in the field based on the aggregation of multiple simulations performed across a range of exposure conditions (in this case, based on variations in ΔV).

Rib Fracture Prediction Method

Rib Cortical Bone Ultimate Strain and Age Adjustment

The first step in this process was to establish a relationship between strain observed in FE model ribs and a risk of fracture. For this analysis, the strain-failure relationship was defined based on the probability that local strains observed in the ribcage model would exceed the ultimate strain of rib cortical bone. This was estimated based on a cumulative distribution of rib cortical bone ultimate strains derived from experimental data available in the literature.

Kemper et al. (2005; 2007) described ultimate strain values obtained through uniaxial tensile testing of coupons of human rib cortical bone. In aggregate, those studies contain tests on specimens from 12 individual cadavers (age 18-81), with 5-20 specimens per cadaver. Because different numbers of tests were performed per cadaver, a mean value of ultimate strain was calculated for each subject. Those mean values were then ranked and combined to determine a

cumulative, non-parametric distribution of mean ultimate strains (Figure 2a).

The ultimate strain cumulative distribution was adjusted to correct for age variations within the Kemper et al. sample group, and to predict fracture risk as a function of age. Through a series of experiments with rib segments, Carter and Spengler (1978) found that the ultimate strain of rib cortical bone decreased with increasing age. They found that, on average, the ultimate strain tends to decrease by approximately 5.1% for each decade of life (with a base age group of 20-29 years). Assuming that age 25 represents the age group 20-29, this relationship may be approximated with a linear model as follows:

$$\varepsilon_{ult}(age) = \varepsilon_{ult25}(1-(age\ -25)\frac{0.051}{10}) \qquad [1]$$

Where $\varepsilon_{ult}(age)$ is the ultimate strain as a function of age and ε_{ult25} is the ultimate strain at age 25.

Rearranging this, it is possible to predict a modified ultimate strain $\varepsilon_{ult,mod}$ at an arbitrary target age (age_{mod}) from an original ultimate strain value ($\varepsilon_{ult,\ original}$) and a corresponding original age ($age_{original}$):

$$\varepsilon_{ult,\mathrm{mod}} = \varepsilon_{ult,original}\frac{(1-(age_{\mathrm{mod}}-25)\frac{0.051}{10})}{(1-(age_{original}-25)\frac{0.051}{10})} \qquad [2]$$

To adjust the fracture prediction analysis by age, each of the entries in the ultimate strain distribution (Figure 2a) were modified by Eq. 2 targeting a single modified age. The resulting modified ultimate strain values were then combined into a cumulative ultimate strain distribution representing said target age (e.g., Figure 2b, c). The resulting modified cumulative distributions tended to show decreased ranges of ultimate strain values compared to the unmodified data, suggesting that this age adjustment removed some of the inter-subject variation from the cadaver test sample.

Predicting Fracture Risks at Individual Locations

The practical interpretation of the ultimate strain cumulative distribution is as follows: the distribution indicates the probability that a chosen strain value is greater than or equal to a randomly-chosen ultimate strain value from within the age-adjusted database (Figure 3). If it is assumed that a fracture occurs whenever the peak strain is greater than or equal to the ultimate strain, then this cumulative distribution can be used to indicate a probability of fracture for a given peak strain.

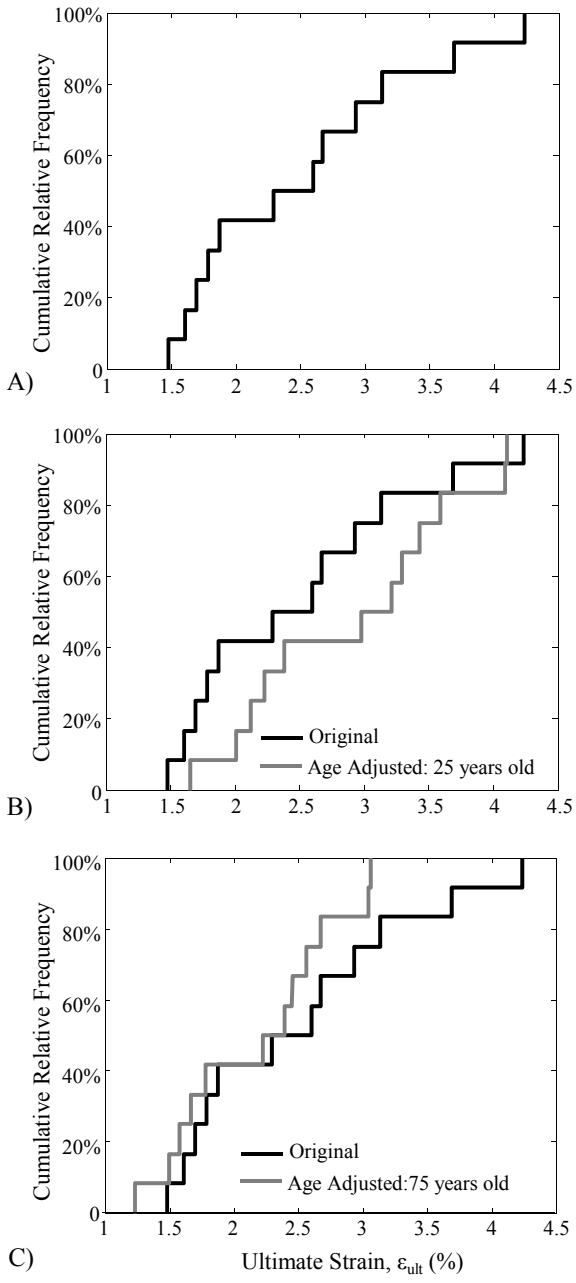

Figure 2: Non-parametric, cumulative relative frequency distributions of rib cortical bone ultimate strains (intra-subject means). A) Original distribution derived from the cadaveric tissue tensile coupon tests of Kemper et al. (2005, 2007) (12 cadaver subjects). B and C) The original distribution compared to age-adjusted examples representing persons age 25 years (B) and 75 years (C).

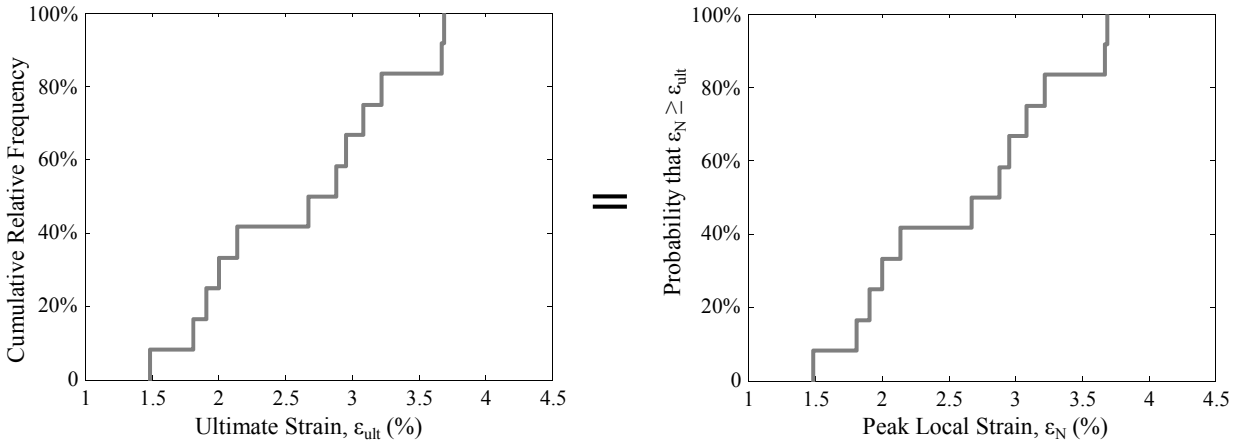

Figure 3: Illustration of the notion that the cumulative relative frequency distribution of rib cortical bone ultimate strains (ε_{ult}) is equivalent to a risk function describing the probability that a chosen peak local strain (ε_N) meets or exceeds the ultimate strain from a subject randomly chosen from the sample group. The plots shown are age-adjusted to estimate an ultimate strain distribution for age 45 years.

For this analysis, peak strain values were observed and organized based on a definition of "potential fracture sites" (or "sites") within the ribcage. These "potential fracture sites" can either be defined as whole individual ribs, or they can be defined based on local areas of peak strain ("hotspots") within the ribs (Figure 4). When the potential fracture sites are defined as whole individual ribs, the analysis is based on the peak strain observed in each rib. In that case, the analysis predicts the number of ribs expected to fracture.

When the analysis is based on "hotspots" (i.e., local strain maxima), the analysis predicts the number of total rib fractures that are expected to occur, with the potential for multiple fractures within individual ribs. In that case, hotspots are identified via a combined quantitative and subjective examination of the strain pattern. First, the strain distribution may be discretized via coarse color mapping with a chosen threshold for coloring (Figure 4). In some cases this results in the appearance of distinct local maxima which can be objectively identified as hotspots (e.g., ribs 7-10 in Figure 4). In some cases, however, the local strains are spread over such an area that a subjective judgment must be made to decide whether a distributed area of maximum strain represents one potential fracture site, or several adjacent potential fracture sites (e.g., rib 4 in Figure 4).

The probability of fracture (p_N) at each site (defined based on either whole ribs or hotspots) was estimated based on a mapping (table lookup) between the peak strain at each site (ε_N) and the cumulative ultimate strain distribution adjusted to a particular age (e.g., Table 1). For the preliminary analyses shown here, only the strains in ribs 1-9 were considered.

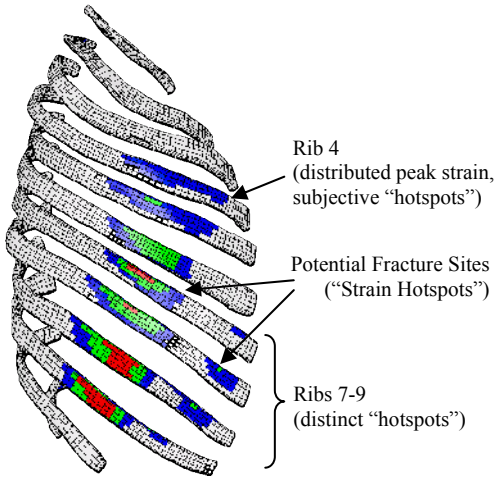

Figure 4: Example color contour plot showing a strain map in the ribs of a whole-body FE model subjected to a frontal collision while restrained by a three-point belt (lateral view of the right ribcage). Potential fracture sites may either be defined as whole ribs (studying the peak strain in each rib), or based on areas of local strain maxima (strain "hotspots").

Table 1: Tabulation of the peak rib strains observed in an example simulation, with the associated probability of fracture at each location (rib or hotspot). (Illustration based on Figure 3.)

"Site" (Rib or Hotspot) #	Peak Strain	Prob. Peak Strain ≥ ε_{ult}
1	0.5	0.00
2	2.5	0.41
3	1.5	0.09
4	3.0	0.59
5	3.0	0.59
6	3.5	0.83
…	…	…
N	ε_N	p_n

Predicting Fracture Risks in the Whole Ribcage

After determining the probability of fracture at each potential fracture site, those probabilities were aggregated to determine the probability of a chosen number of fractures occurring in the entire ribcage (Pr(*X*)). This was accomplished using a generalized form of a binomial probability model:

$$\Pr(X) = \sum_{i=1}^{\binom{N}{X}} \left(\prod_{j \in \mathbf{C}_i} p_j \right) \left(\prod_{k \in \overline{\mathbf{C}}_i} (1 - p_k) \right) \qquad [3]$$

Where:

Pr(X) is the probability of observing exactly X fractures in the ribcage

p_j is the probability of fracture at the j[th] site (rib or hotspot number)

N is the number of potential fracture sites (number of ribs or hotspots studied)

$\mathbf{C}_i$ is a vector containing the i[th] combination of X site indices

$\overline{\mathbf{C}}_i$ is a vector containing the set-exclusive-or values between the index vector [1…N] and the combination vector $\mathbf{C}_i$

And where $\binom{N}{X}$ is the binomial coefficient:

$$\binom{N}{X} = \frac{N!}{X!(N-X)!} \qquad [4]$$

Equation 3 was used to determine cumulative probability distributions for the number of fractures predicted to occur for a given simulation (e.g., Figure 5a). This information was used to determine point estimates and 90% confidence intervals (C.I.) for the number of predicted fractures. The point estimate was defined as the fracture number crossing a 50% cumulative probability (the first fracture number meeting or exceeding 50%). The confidence interval lower bound and upper bound were defined as the fracture numbers crossing cumulative probabilities of 5%and 95%, respectively (Figure 5a). When this analysis is repeated for different target ages, it is possible to estimate how the point estimates and C.I. for the predicted number of fractures change with age (Figure 5b).

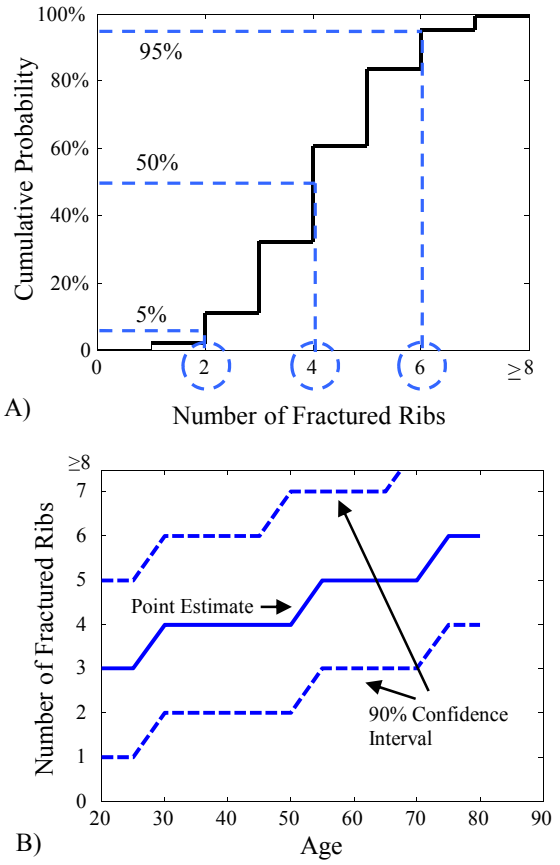

Figure 5: A) Illustration of the determination of the point estimate and 90% confidence interval (C.I.) for the number of fractures predicted to occur from an example simulation. In this case, the C.I. would be 2 to 6 fractured ribs, with a point estimate (50[th] percentile value) of 4. B) Illustration of the relationship between age and the number of fractured ribs predicted to occur for an example simulation.

In addition to determining the probability of observing exactly X fractures, it is often desirable to determine the probability of incurring greater than or

equal to a chosen number of fractures (i.e., ≥Y fractures). This was determined by summing the probabilities of observing 0 to Y-1 fractures, then finding the probability compliment:

$$P_{\geq}(Y) = 1 - \sum_{X=1}^{Y-1} \Pr(X) \qquad [5]$$

Where: $P_{\geq}(Y)$ is the probability of observing ≥Y fractures, and $Pr(X)$ is the probability of observing exactly X fractures, as defined by Eq. 3.

The analysis to this point has assumed that rib fractures are independent events, where the occurrence of a fracture in one location does not affect the probability of fracture in another location. This is assumed to be true for cases with relatively low numbers of rib fractures, where the structural integrity of the ribcage remains intact. There is some experimental evidence to support this assumption – several studies have indicated that the overall stiffness of the chest remains relatively consistent under diagonal belt loading (Kent et al., 2004) even with rib fractures that meet or exceed a severity of AIS 3 (Kemper et al., 2011) or AIS 4 (Duma et al., 2011). Large numbers of rib fractures, however, have the potential to destabilize the ribcage, potentially affecting the risk of fracture at other sites. Because of this, this analysis limited the calculation of distinct probabilities of fracture to cases of 0 to 7 fractures. If the point estimate, upper, or lower bounds did not fall within the range of 0-7 fractures, then they were defined to be ≥8 fractures (but were not specified further, e.g., Figure 5b).

Sensitivity Analyses & Preliminary Validation

Finite Element Model

Preliminary evaluations of the rib fracture prediction method were performed with a modified version of the THUMS (Total Human Model for Safety) 50th percentile male, whole-body finite element model (Toyota Central R&D LABS Inc., 2005). The original THUMS model was updated with a number of in-house modifications. The complete chest was remeshed with an increase in the number of nodes and elements. The ribs were modeled using a combination of solid and shell elements. For the complete original THUMS the number of nodes and elements were 66617 and 87282 respectively; for the complete modified THUMS the number of nodes and solid elements were 110,100 and 156,522 respectively. The ribs of the original THUMS consisted of 1022 shell elements and 3128 solid elements. The ribs of the modified THUMS consisted of 18512 shell elements and 15276 solid elements. The cortical bone making up the perimeter circumference of the rib cross-section was comprised of a single layer of shell elements. In the original THUMS there was a failure criterion defined for the cortical bone which was excluded in the modified THUMS. Rhomboid muscle elements (that were absent in the original THUMS) were also added to improve shoulder and arm kinematic biofidelity.

The material model used for the modified THUMS ribs was an elasto-plastic model. For the cortical bone the Young's modulus was 10.2 GPa, yield stress was 65 MPa. For the trabecular bone the Young's modulus was 40 MPa, and the yield stress was 1.8 MPa. No strain-rate dependency was defined. The spinal column vertebrae were modeled with rigid bodies connected by spring elements. The intervertebral disks were modeled with an elastic material model. The ligaments were represented by spring elements. Biofidelity validation analyses of the modified THUMS chest have been previously reported under both whole-body, collision-type restraint loading (Pipkorn and Mroz, 2008) and in component-level evaluations (Pipkorn and Kent, 2011).

Number of Elements to Define Fracture

This analysis is based on the peak strain observed at each potential fracture location (or within each rib). There remains, however, different methods that may be used to define "fracture" based on local strains. In the simplest case, the initiation of fracture (e.g., cracking) could be defined to occur when any single element exceeds a strain threshold. In contrast, fracture could be defined as a gross structural failure predicted to occur when several adjacent elements exceed a strain threshold. For example, this type of definition might require that all adjacent elements along one edge of the perimeter of the rib cross-section (i.e., on the surface of the rib) must exceed a strain threshold before a fracture is expected to occur. In the modified THUMS model used here, this would require approximately 5 adjacent cortical bone elements to exceed the strain threshold.

A series of cases were analyzed to study the sensitivity of this method to the number elements used to define a fracture. Three different levels of fracture definitions were considered, defining fracture as occurring when: A) any one element exceeds a strain threshold; B) three adjacent elements exceed a strain threshold; and C) five adjacent elements exceed a strain threshold. The 1-element and 5-element definitions were chosen based on the bounds of the discussion above, with the 3-element definition chosen as an intermediary.

This analysis was performed for two different simulation conditions. Both consisted of 48 km/h frontal impacts with the modified THUMS model. In simulation Condition A, the occupant model was restrained by a progressively force-limited (3 kN to 7 kN), pre-tensioned 3-point seatbelt (FL+PT belt). In simulation Condition B, the occupant model was restrained by a standard (not force-limited or pre-tensioned) 3-point seatbelt. The simulation environment (seat and restraint geometry, acceleration pulse) was modeled after the frontal-impact, rear seat occupant sled tests reported by Forman et al. (2009).

Fractured Ribs versus Rib Fractures

As discussed above, it is possible to base these analyses either on the number of ribs predicted to fracture (defined by the peak strain in each rib), or based on the number of rib fractures predicted to occur (with the potential for multiple fractures per rib). Because it is based simply on the peak strain in each rib, studying the number of fractured ribs is objective, unambiguous, and easy to define and execute. In contrast, studying the number of rib fractures requires a subjective judgment as to what constitutes a potential fracture site. Often, strain hotspots are close enough to each other to merge, with no clear boundary or indication whether or not multiple distinct fracture sites may exist (Figure 4). In addition, even if multiple distinct hotspots are observed for a given strain threshold, if close enough those hotspots can merge into a single large hotspot as the strain threshold decreases. If implemented without a qualitative check, this can lead to a paradoxical result wherein the number of potential fracture sites decreases as the strain threshold decreases. For objectivity and ease of execution, it is desirable to limit our analysis to the study of the number of fractured ribs predicted to occur (via the peak strain per rib). An analysis was performed to study the sensitivity of defining injury based on whole ribs versus individual hotspots. This analysis was performed for the same two simulation conditions used for the element number sensitivity analysis described above.

Preliminary Validation – Comparison to Whole-Body Sled Tests

The analysis method developed here provides a theoretical framework for the interpretation of rib cortical bone strains from finite element simulations. To be useful as a tool to predict injury, the accuracy of this analysis method must be validated. While an in-depth validation is beyond the scope of the current study, we can begin to explore the accuracy of the method by comparing the results to existing experimental data.

Three simulations were performed to represent conditions similar to frontal impact, cadaver sled tests described previously. A 29 km/h, frontal impact, simulation with a standard 3-point belt was performed to match the conditions of the three cadaver sled tests described by Forman et al. (2006). 48 km/h, frontal impact simulations were performed with a standard 3-point belt and a FL+PT belt to match conditions of the cadaver sled tests described by Forman et al. (2009). The overall model responses (shoulder belt force, chest deflection, kinematics) and the predicted rib fracture risks were then compared to the experimental results.

Exposure-Based Field Risk Prediction

The final goal of this study was to describe a method to translate the fracture risks derived from individual simulations into exposure-based field risk estimates. This may be accomplished by 1) establishing a field frequency distribution of exposure variables of interest; 2) calculating simulation-based risk-response curves spanning the range of exposure conditions of interest; and 3) combining the risk-response curves with the field exposure distributions to determine estimates of risk in the field. For the ease of illustration, this study performed a one-dimensional field risk analysis for frontal collisions (with a specific vehicle, restraint, and occupant configuration) using ΔV as the exclusive exposure variate.

Field-Derived Exposure

A field distribution of ΔV for frontal collisions was derived from data reported by Kent et al. (2005a). This distribution shows the cumulative ΔV frequency of all drivers involved in tow-away frontal crashes (PDOF: 11 to 1 o'clock), derived from the NASS-CDS 1992-2002 database (weighted). Detail on the data selection procedures is reported by Kent et al. (2005a). The cumulative ΔV distribution was discretized then converted into a relative frequency distribution with 1 km/h binned increments.

Inter-Condition Response Surfaces

Instead of performing simulations at each possible value of ΔV, it may be possible to describe the relationship between ΔV and risk using a parametric function fit to the risk values predicted from a finite number of simulations. This simulation-derived parametric relationship is termed a "response surface" (recognizing that this could span multiple dimensions if a multi-variate exposure analysis were performed) (Thacker et al., 1997).

Based on preliminary observations a logistic model was chosen to represent the relationship between ΔV and fracture risk for this study. The form of this model is shown in Equation 6.

$$P_s(\geq Xfx:\Delta V) = \frac{1}{1+e^{-\alpha-\beta(\Delta V)}} \quad [6]$$

Where α and β are model coefficients, and $P_s(\geq Xfx:\Delta V)$ is the response surface describing the probability of incurring ≥X fractures for a given ΔV.

For the two restraint conditions studied here (standard belt and FL+PT belt), simulations were performed at four levels of ΔV: 29, 35, 42 and 48 km/h. For each age & restraint condition combination, the logistic model coefficients were optimized to best fit the relationship between ΔV and fracture risk. This analysis was automated (using custom code in MatLab) to determine response surfaces across ages ranging from 20 to 85 years.

Aggregation into Field Risk Prediction

Finally, the field exposure distribution was combined with the simulation-derived response surfaces (P_s) to estimate the risk of injury in frontal tow-away collisions with this vehicle, occupant, and restraint configuration in the field. For a discretized analysis, this is accomplished via the weighted summation shown in Equation 7 (Laituri et al., 2009):

$$P(\geq Xfx) = \sum_i P_{rf}(\Delta V_i) * P_s(\geq Xfx:\Delta V_i) \quad [7]$$

Where $P(\geq Xfx)$ is the probability of ≥X fractured ribs in the field, P_{rf} is the relative frequency distribution of ΔV_i, and P_s is the probability ≥X fractured ribs for a given ΔV_i (Equation 6).

RESULTS

Sensitivity Analyses

Figure 6 shows the results of the sensitivity analysis performed to study the effect of the number of elements used to define fracture. These plots show the probability of ≥3 and ≥7 fractured ribs by age for 48 km/h frontal collision simulations with a standard belt and a FL+PT belt, where fractures are defined as occurring when ≥1, ≥3, or ≥5 adjacent elements exceed the ultimate strain of the rib bone.

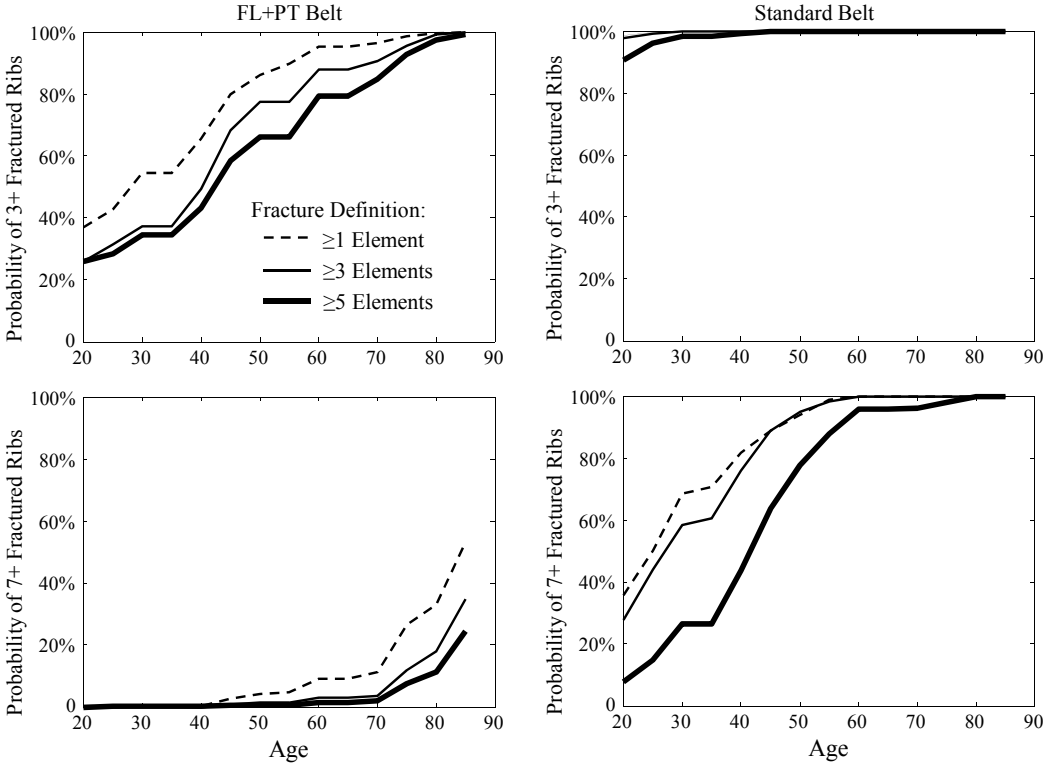

Figure 6: The effect of the number of adjacent elements used to define fracture on the predicted probability of fractured ribs in simulated 48 km/h frontal impact collisions. Top: Predicted probability of incurring 3+ fractured ribs with age. Bottom: Predicted probability of incurring 7+ fractured ribs. Based on simulations with a standard 3-point belt (right) or progressive (3-7 kN) force-limiting, pretensioning (FL+PT) belt (left).

Figure 7 shows the results of the sensitivity analysis studying the effect of defining injury in terms of the numbers of fractured ribs (via the peak strain per rib) versus the total number of rib fractures (via individual hotspots, with the possibility of multiple fractures per rib). The results show very little sensitivity, with the only discernible difference occurring when predicting the probability of 7+ fractures with the standard belt condition. For the other conditions predicting the number of fractures via the peak strain per rib produced indiscernible results compared to predicting fracture via hotspots with the possibility of multiple fractures on individual ribs.

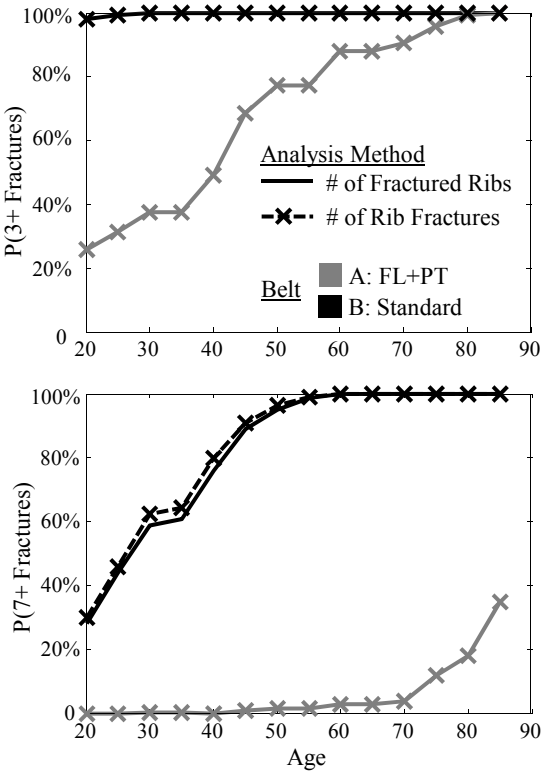

Figure 7: Results of the sensitivity analysis studying the effect of predicting the number of fractured ribs (via the peak strain per rib) versus the number of rib fractures (via the peak strain per hotspot, with the potential for multiple fractures per rib). Note that the "fractured ribs" and "rib fractures" analyses produced indistinguishable results for all cases except when predicting 7+ fractures in the standard belt condition.

Comparison to Sled Test Data

Table 2 shows the peak upper shoulder belt force (F_{max}) and peak normalized mid-sternal chest deflections (C_{max}) of the three simulations that were compared to matched cadaver sled tests. The F_{max} values have been scaled by the subject mass (explained in detail by Forman et al. 2009) to estimate the forces that would be experienced by a 50th percentile male (target occupant mass: 77 kg). The model C_{max} values compared reasonably well (within ± one standard deviation) to the experimental results. The scaled upper shoulder belt forces of the sled tests were consistently lower than the simulation values. Figure 8 shows still captures of lateral views of the models and experiments at the time of maximum forward head excursion. As with the C_{max} values, the overall kinematics of the models and the experiments qualitatively compared reasonably well.

Figure 9 shows a comparison of the fractures observed in the experiments to the numbers of fractured ribs predicted by the analysis of matched simulations. The simulation results include 90% confidence intervals and predicted variations with age.

Table 2: Simulation peak responses compared to matched experiments (average ± standard deviation)

		F_{max} (kN)*	C_{max} (%)†
29 km/h Standard Belt	Model	5.2	15
	Experiment	4.0±0.5	15±7.5
48 km/h FL+PT Belt	Model	6.5	25
	Experiment	4.4±0.1	27±7
48 km/h Standard Belt	Model	8.9	30
	Experiment	7.8±0.6	28±4

* Peak upper shoulder belt tension, scaled by subject body mass to a 77 kg reference (Forman et al., 2009).

† Peak displacement of the external surface of the chest towards the spine, measured at the mid-sternum at the superior-inferior location of the 4th rib, as a percentage of the initial chest depth (Forman et al., 2009).

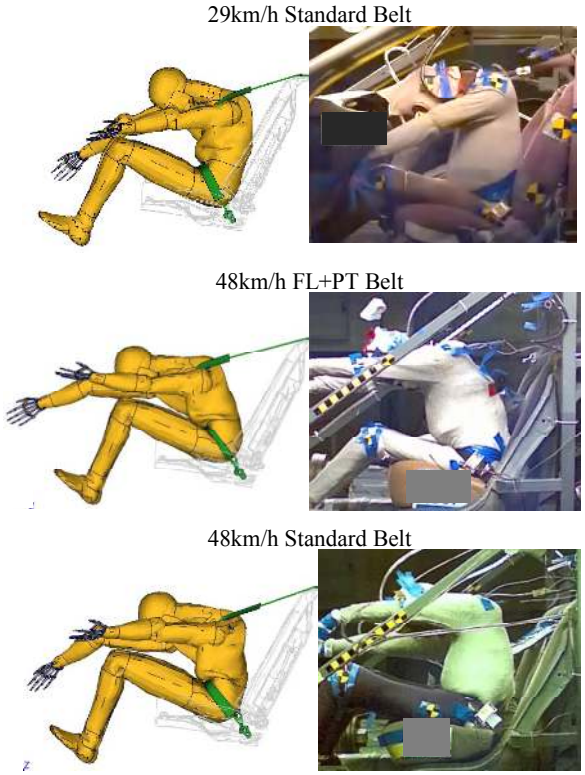

Figure 8: Still images of simulations (left) compared to typical matched cadaver tests (right) at the time of maximum forward head excursion. (Note: The shoulder belt passed over the left shoulder in the simulations and the right shoulder in the experiments. The experiment still images were taken from the occupant's right side and mirrored to allow a consistent comparison with the simulations. Images not to scale.)

ΔV Response Surfaces and Field Risk Prediction

Figure 10 shows the cumulative distribution and discretized relative frequency distribution of ΔV of drivers involved in frontal collisions (PDOF: 11-1 o'clock), NASS-CDS 1992-2002 (Kent et al., 2005a). The relative frequency histogram is truncated at 20 km/h based on a preliminary observation (from the simulation analysis) of approximately zero risk of rib fracture injury at ΔV values less than 20 km/h.

Figure 11 shows several examples of discrete risk estimates derived from simulations performed across a range of ΔVs, and the logistic regression response surfaces (curves) fit to describe those data. Examples are shown of simulations performed with a standard belt, analyzed to predict various severities of fracture risk (3+ fractures, 7+ fractures) for two illustrative ages.

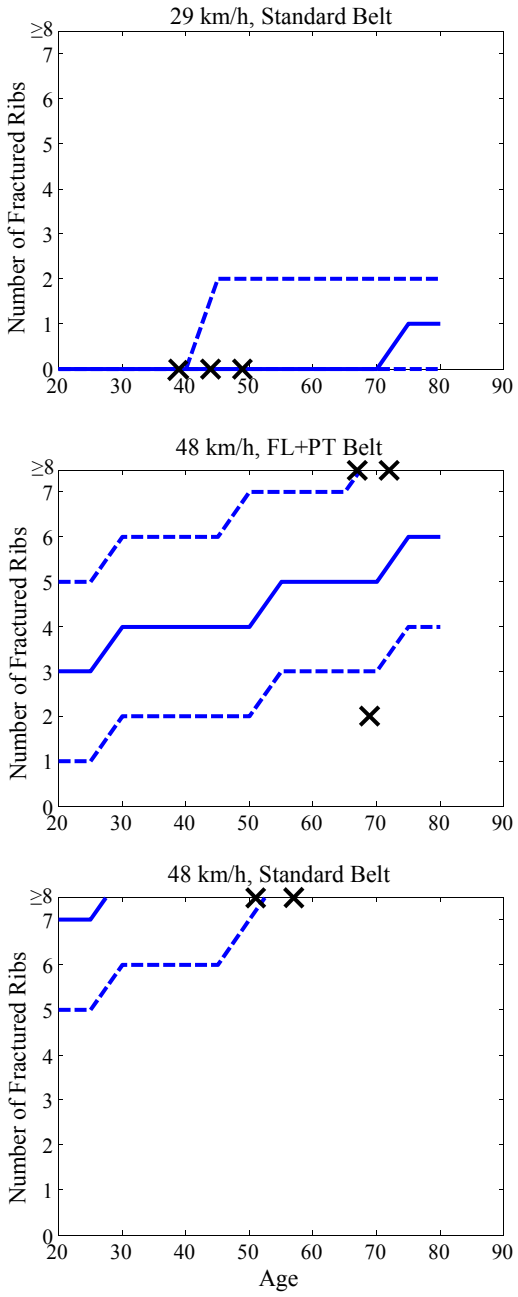

Figure 9: The number of fractured ribs observed in frontal-impact cadaver sled tests (shown as black X's) compared to the point-estimates and 90% C.I. of the number of fractured ribs predicted to occur via analysis of simulations performed in matching conditions (shown as blue lines).

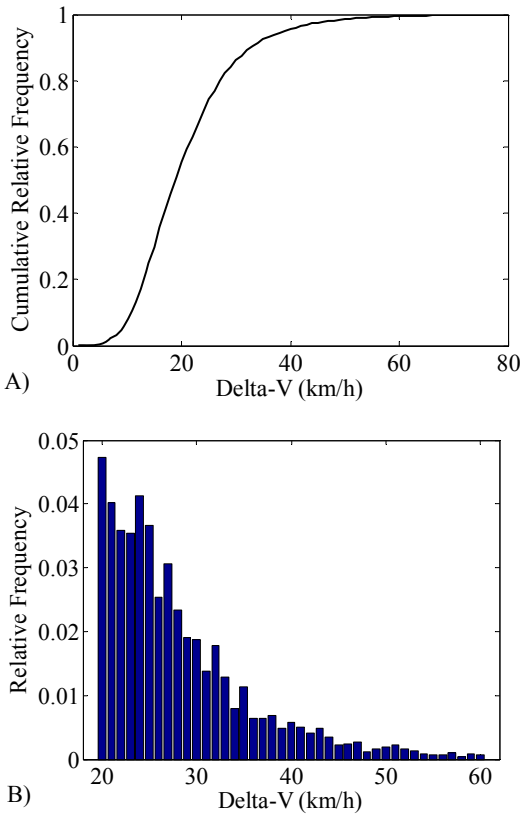

Figure 10: A) Cumulative relative frequency distribution of ΔV of drivers (age 16+) involved in tow-away frontal collisions, NASS-CDS 1992-2002 (PDOF 11-1 o'clock, weighted; Kent et al., 2005a). B) Discretized relative frequency distribution of ΔV derived from plot A (1 km/h increments, 20-60 km/h).

Figure 12 shows the resulting field risk estimations generated by combining the field ΔV exposure data of Figure 10b with the risk response surfaces generated through the simulation analyses. Field risks were estimated for the probability of 3+ fractured ribs, by age. This analysis suggests a 8.9% probability of incurring 3+ fractured ribs for a 60 year old restrained by a standard belt in a frontal collision (for this vehicle, restraint, and occupant configuration), compared to 4.6% for the progressive FL+PT belt system studied here.

DISCUSSION

Sensitivity Analyses

As expected, the predicted probability of fracture was dependent on the number of elements used to define fracture (Figure 6). This effect was small, however, compared to the differences observed between the two restraint conditions studied here. This analysis gives an indication of the potential range of error to expect due to continued uncertainty regarding how to best predict fracture on a material level. Future work should include studying this definition through smaller-scale experiments (e.g., with individual ribs) to increase the precision of fracture prediction.

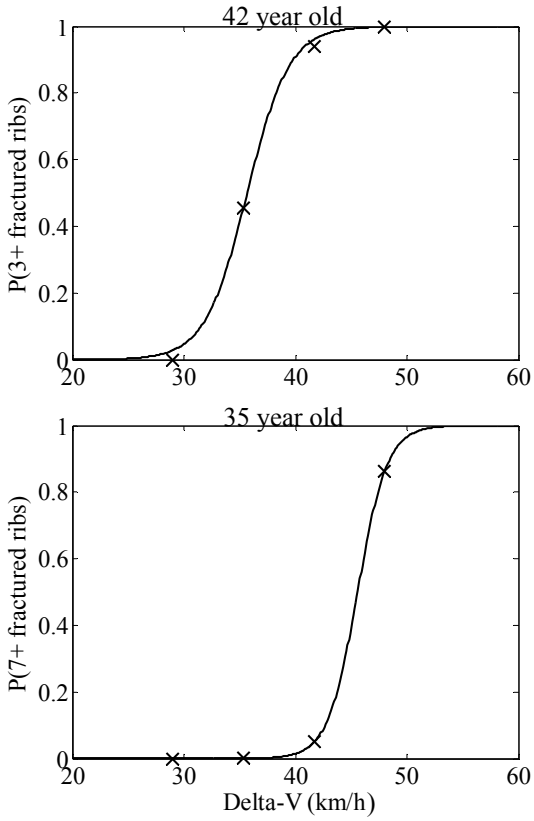

Figure 11: Illustration of the injury risk curves derived from example simulations performed at discrete values of ΔV (29, 35, 42, and 48 km/h). The discrete model results are shown as X's; logistic response curves are shown as solid lines. Two examples are shown: probability of 3+ fractured ribs for a 42 year old (top); and probability of 7+ fractured ribs for a 35 year old (bottom), both for frontal collisions with a standard 3-point belt.

In contrast to the element definition sensitivity, the analysis results (in the cases studied) were relatively insensitive to basing the analysis on the peak strain observed in each rib versus studying individual hotspots (Figure 7). Only one condition (the predicted risk of 7+ fractures with a standard belt) showed any sensitivity. In that case the probability based on the individual hotspots (the total number of "rib fractures") was slightly greater than the probability based on the peak strain per rib (the number of "fractured ribs"). That difference was small, with a maximum error of approximately five percentage points. As a result, due to the ease of execution it may be appropriate to base future similar

analyses on the number of fractured ribs predicted to occur via studying the peak strain in each rib.

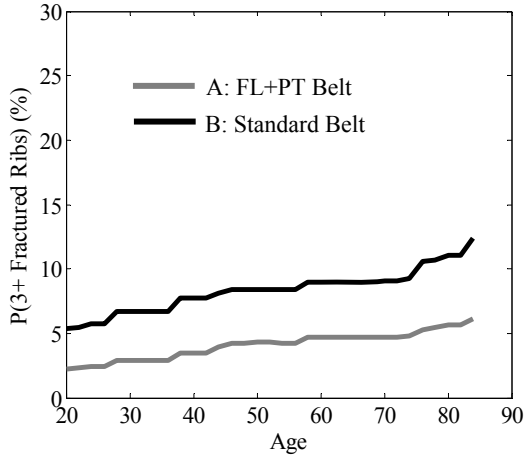

Figure 12: Predicted risk of incurring 3+ fractured ribs during a tow-away frontal collision (with this vehicle, restraint, and occupant configuration), by age, for a person restrained by a standard 3-point belt or a progressive (3-7 kN) force-limited, pretensioned (FL+PT) 3-point belt.

Comparison to Experimental Data

As shown in Figure 9, the confidence intervals for the numbers of fractured ribs predicted by the simulation analysis agreed relatively well with the experimental data. The number of fractures observed within the experiments fell within the 90% confidence intervals for all but one case. The chest deflections and overall kinematics of the simulations compared well to the experiments. The scaled upper shoulder belt forces differed somewhat, appearing consistently lower in the experiments compared to the simulations. This, however, appears to have had limited effect on the injury risk prediction comparison given that the chest deformations, trends (ranking) of belt forces, and predicted vs. observed rib fractures remained relatively consistent between the simulations and experiments. These results, although limited in sample size, support the notion that the simulation analysis method can discriminate differences in fracture risk in a manner relatively consistent with experimental data. Consistent with the experimental results, the simulation analyses predicted a very low probability of fractures for the 29 km/h standard belt condition and a very high probability of many (8+) fractures for the 48 km/h standard belt condition. The 48 km/h, FL+PT condition fell between those two extremes, with both the simulation analysis and the experimental results indicating a relatively wide range of possible injury severities. These results suggest that the analysis method can distinguish between conditions very likely to cause many rib fractures (48 km/h, standard belt), conditions very unlikely to cause any fractures (29 km/h standard belt), and conditions closer to the injury threshold where there will be some range of probabilities of fracture (48 km/h, FL+PT belt).

Practical Implications and Field Risk Prediction

This is the first study (to the authors' knowledge) to develop a strategy for causal, probabilistic thoracic injury prediction using human body FE models. While a preliminary study, the framework developed here may provide a base for future refinement of FE based injury prediction. These methods are not limited to thoracic injury, but could also be applied to other body regions or injury types.

The methods developed here also provide a means to estimate field injury risk and the potential impact of countermeasures in a manner not possible with deterministic methods. Deterministic methods predict the occurrence of injury in a specific individual. As a result, they are limited in their ability to represent injury occurrence in a population. The probabilistic methods described here allow the study of injury risk across a population with varying characteristics. These methods also allow the development of injury probability curves across a range of collision conditions, using a parametric simulation strategy not often possible with physical crash tests. When combined with exposure information, these types of risk response curves may allow the prediction of injury in the field, or the prediction of the potential impact of countermeasure strategies.

It should be noted that the preliminary analysis described here was based on a single vehicle, collision, and restraint environment (aside from changing ΔV) and a single occupant anthropometry. As a result, the field risk predictions shown in Figure 11 are not directly comparable to field risks observed in the entire fleet. Instead, the results shown here are intended as a preliminary illustration of how this type of analysis may be used to study potential differences between restraint systems across a chosen distribution of collision characteristics. The predicted risks shown in Figure 11 are, in general, greater than the observed risks of AIS 3+ thoracic injury typically reported in the literature for belted occupants in frontal collisions (Laituri et al., 2009; Kuppa et al., 2005). This may be the result of variations in vehicle, occupant, restraint, or collision characteristics in the fleet. This may also be an indication of limitations in the modeling methods, consistent with the observance of greater shoulder belt forces in the simulations compared to the matched cadaver sled tests. Confounding factors are not limited to the

modeling or analysis methods however – comparisons to field data may also be effected by limitations in the diagnosing or reporting of individual rib fractures (Kent et al., 2002; Oberladstaetter et al., 2012). Further validation efforts are needed to identify and correct any potential sources of error. Using the concepts described here this type of analysis could be expanded to include multi-variate vehicle, collision, and occupant characteristics, and other types and combinations of restraints (e.g., combined belt and airbag systems).

Limitations and Future Work

Ribcage Stability and Fracture Event Independence
This analysis assumed that each fracture was an independent event, where a fracture at one site does not affect the probability of fracture at another site. Some evidence exists suggesting that small to moderate numbers of rib fractures have little effect on the overall stiffness of the chest (Kent et al., 2004; Duma et al., 2011; Kemper et al., 2011). Because of this, this study limited the prediction of incremental changes in the number of rib fractures to the range of 0-7 fractures, with anything more being lumped into a greater severity category of 8+ fractures. Studying distinct fracture occurrence after ribcage destabilization (whatever the threshold) would require the use of a frangible FE model implementing probabilistic methods in the simulation matrix design.

In addition, this topic should be considered in the context of the utility of chest injury prediction tools in general. From a clinical perspective, there may be some threshold for the number of rib fractures over which incremental changes have little effect on the outcome (for example, if a person has a severe flail chest then it may make little difference if that occurred as a result of 10 rib fractures or 12 rib fractures). Thus, instead of thinking of rib fractures as a continuous variable, it may be more appropriate to think of rib fractures as a measure of overall injury severity with thresholds separating lower-severity and higher-severity cases (with the potential for multiple intermediate thresholds depending on the desired usage). This is exactly how injury prediction methods are implemented practically – a threshold for injury severity is specified and then a method is developed to predict the risk of exceeding that threshold (for example, incurring ≥8 fractures).

Even in the absence of ribcage destabilization, the degree to which rib fractures influence strain in other ribs is unknown. Future work should include investigating the validity of the rib fracture independence assumption. This could be accomplished computationally by performing a simulation with element elimination or softening models to simulate fracture, then studying the effect of fractures on the peak strains in adjacent ribs. Such a method could also be used to determine an upper limit (in terms of the number of fractures) for which the independence assumption is valid.

Ultimate Strain Independence
This work also assumed that the ultimate strain values for each location in the ribcage were independent from values in other locations, all following the age-adjusted ultimate strain distributions described above. It is likely, however, that there exists some intra-subject dependence in ultimate strain. Future work may include investigating the effect of incorporating intra-subject dependence in ultimate strain. This could include a hybrid-type model, with a distribution defining the inter-subject variation in mean ultimate strain in the population, combined with knowledge on typical intra-subject variations about that mean within an individual ribcage.

Ultimate Strain Database
This analysis was based on a database of mean ultimate strain values from twelve cadaveric subjects (Kemper et al., 2005; Kemper et al., 2007). Although the subjects exhibited a wide range of ages (18 to 81), the small number of subjects may limit the dataset as a representation of the entire population. Future work should include expanding this database to improve both the resolution and the accuracy of the ultimate strain distribution used in this analysis.

Other Variables
This preliminary analysis studied variations in rib fracture risk based on variations in the ultimate strain of rib cortical bone. This was chosen in part because ultimate strain can be explored probabilistically post-simulation, without the need to perform additional simulations with altered models. There are several other factors that vary in the population that may affect rib fracture risk. These include rib-cage specific properties such as cortical bone thickness, cortical bone elastic modulus, and ribcage geometry (Kent et al., 2005b). These also include other subject factors that may affect chest loading, such as body mass and mass distribution. Future work could include adding probabilistic models of those variables to the analysis framework presented here.

The exposure analyses shown here were based on variations in one variable (ΔV). This can be expanded to include other variables (either in collision exposure or in occupant characteristics)

with the same basic strategy. The results would include multi-variate response surfaces which could then be combined with exposure or population information. The dimension (number of variables) of such analyses would only be limited by the number of simulations required to adequately define the response surfaces in the multi-dimensional space.

Validation

To be useful as a tool to predict injury, the accuracy of the analysis method described here must be validated. The comparisons to sled test data in Figure 8 provide a beginning to the validation effort. Those comparisons are limited, however, by low sample sizes and by potential confounding factors such as the FE model biofidelity and the individual experimental subject characteristics. Future work should expand these validation efforts to identify potential sources of error in the overall injury prediction strategy. This would ideally include a multi-tiered approach, validating multiple steps in the simulation and analysis process to identify and eliminate potential sources of error (for example, evaluating the model biofidelity by comparing the simulation strains to strains measured experimentally). This could also include simulating and predicting injury risk under simplified boundary conditions for which larger numbers of experimental data points are available (for example, blunt hub loading).

CONCLUSION

This study described a causal probabilistic framework for the prediction of rib fracture risk using strain outputs from human body FE models. This method incorporated variations in rib cortical bone ultimate strain, and included a method to predict changes in rib fracture risk with age. Preliminary sensitivity analyses indicated that the prediction of fracture risk was sensitive to the number of elements used to define fracture, but that effect was less than the effect of the different restraint conditions studied. The results were relatively insensitive to the study of the number of fractured ribs (via the peak strain per rib) versus the number of rib fractures (with the possibility of multiple fractures per rib). Results with a modified version of the THUMS model were relatively consistent with injury severities observed in matched cadaver sled tests under three test conditions (frontal impact - 29 km/h with a standard belt; 48 km/h with a progressive force-limiting, pre-tensioning belt; 48 km/h with a standard belt). Although preliminary, those analyses suggest that this method may be able to distinguish between conditions with a very low probability of injury, conditions with a very high probability of severe injury, and conditions near the risk transition in a manner consistent with experimental data. This study also described a method to combine the results of multiple simulations performed across collision conditions into risk response surfaces, and to combine those response surfaces with exposure information to estimate field injury risk for a particular vehicle, restraint, and occupant configuration.

This study represents a framework, or strategy, for probabilistic injury prediction with FE models of the human body. Future work includes exploring this framework with multi-variate probabilistic injury prediction, both with other subject characteristics and other collision exposure characteristics. Future work also may include exploring other methods for combining local fracture probabilities to predict injury severity in the whole ribcage. Future work should also include continued efforts in validation, including multi-level simulation validation and studying the level of subject-characteristic precision needed to accurately predict injury risk.

ACKNOWLEDGMENTS

This study was supported in part by Autoliv Research, and by a Whitaker International Scholars Grant. The opinions presented here are solely those of the authors, and do not necessarily represent the consensus views of the funding organizations.

REFERENCES

Carter, D. R., Spengler, D. M., (1978). Mechanical properties and composition of cortical bone. Clin.Orthop.Relat Res. 192-217.

Duma, S., Stitzel, J., Kemper, A., McNally, C., Kennedy, E., Brolinson, G., Matsuoka, F., (2006). Acquiring non-censored rib fracture data during dynamic belt loading. Biomed.Sci.Instrum. 42**,** 148-153.

Duma, S. M., Kemper, A. R., Stitzel, J. D., McNally, C., Kennedy, E. A., Matsuoka, F., (2011). Rib fracture timing in dynamic belt tests with human cadavers. Clin Anat 24**,** 327-338.

Forman, J., Lopez-Valdes, F., Lessley, D., Kindig, M., Kent, R., Ridella, S., Bostrom, O., (2009). Rear seat occupant safety: an investigation of a progressive force-limiting, pretensioning 3-point belt system using adult PMHS in frontal sled tests. Stapp Car Crash Journal 53**,** 49-74.

Forman, J., Lessley, D., Shaw, C. G., Evans, J., Kent, R., Rouhana, S. W., Prasad, P., (2006). Thoracic

response of belted PMHS, the Hybrid III, and the THOR-NT mid-sized male surrogates in low speed, frontal crashes. Stapp Car Crash J. 50**,** 191-215.

Francis, W. L., Bonivitch, A. R., Moravits, D. E., Paskoff, G. R., Shender, B. S., Bass, C. R., Lucas, S. R., Pintar, F. A., Yoganandan, N., Koebbe, M. H., Thacker, B. H., Nicolella, D. P., (2005). Probabilistic response of a validated and verified parametric cervical spine finite element model. Proc.33rd Int.Workshop on Injury Biomechanics Research.

Kemper, A. R., Kennedy, E. A., McNally, C., Manoogian, S. J., Stitzel, J. D., Duma, S. M., (2011). Reducing chest injuries in automobile collisions: rib fracture timing and implications for thoracic injury criteria. Ann Biomed Eng 39**,** 2141-2151.

Kemper, A. R., McNally, C., Kennedy, E. A., Manoogian, S. J., Rath, A. L., Ng, T. P., Stitzel, J. D., Smith, E. P., Duma, S. M., Matsuoka, F., (2005). Material properties of human rib cortical bone from dynamic tension coupon testing. Stapp.Car.Crash.J. 49**,** 199-230.

Kemper, A. R., McNally, C., Pullins, C. A., Freeman, L. J., Duma, S. M., Rouhana, S. M., (2007). The biomechanics of human ribs: material and structural properties from dynamic tension and bending tests. Stapp Car Crash J 51**,** 235-273.

Kent, R., Henary, B., Matsuoka, F., (2005a). On the fatal crash experience of older drivers. Ann Adv Automot Med.

Kent, R., Lee, S. H., Darvish, K., Wang, S., Poster, C. S., Lange, A. W., Brede, C., Lange, D., Matsuoka, F., (2005b). Structural and material changes in the aging thorax and their role in crash protection for older occupants. Stapp.Car.Crash.J. 49**,** 231-249.

Kent, R., Lessley, D., Sherwood, C., (2004). Thoracic response to dynamic, non-impact loading from a hub, distributed belt, diagonal belt, and double diagonal belts. Stapp Car Crash J. 48**,** 495-519.

Kent, R., Woods, W., Bostrom, O., (2008). Fatality risk and the presence of rib fractures. Annals of Advances in Automotive Medicine 53**,** 73-84.

Kent, R. W., Crandall, J., Patrie, J., Fertile, J., (2002). Radiographic detection of rib fractures: a restraint-based study of occupants in car crashes. Traffic.Inj.Prev. 3**,** 49-57.

Kuppa, S., Saunders, J., Fessahaie, O., (2005). Rear seat occupant protection in frontal crashes.

Laituri, T. R., Henry, S., Kachnowski, B., Sullivan, K., (2009). Initial assessment of the next-generation USA frontal NCAP: fidelity of various risk curves for estimating field injury rates of belted drivers. Society of Automotive Engineers, Paper No.2009-01-0386.

Laituri, T. R., Prasad, P., Sullivan, K., Frankstein, M., Thomas, R. S., (2005). Derivation and evaluation of a provisional, age-dependent, AIS3+ thoracic risk curve for belted adults in frontal impacts. Society of Automotive Engineers Paper Number 2005-01-0297.

Oberladstaetter, D., Braun, P., Freund, M. C., Rabl, W., Paal, P., Baubin, M., (2012). Autopsy is more sensitive than computed tomography in detection of LUCAS-CPR related non-dislocated chest fractures. Resuscitation 83**,** e89-e90.

Pattimore, D., Thomas, P., Dave, S. H., (1992). Torso injury patterns and mechanisms in car crashes: an additional diagnostic tool. Injury 23**,** 123-126.

Pipkorn, B., Kent, R., (2011). Validation of a human body thorax model and its use for force, energy, and strain analysis in various loading conditions. Proc.International Research Council on the Biomechanics of Impact Paper No. IRC-11-56.

Pipkorn, B., Mroz, K., (2008). Validation of a human body model for frontal crash and its use for chest injury prediction. SAE Conference on Digital Human Body Modeling Paper No. 2008-01-1868.

Rahman, S., (2001). Probabilistic fracture mechanics: J-estimation and finite element methods. Engineering Fracture Mechanics 68**,** 107-125.

Thacker, B. H., Wu, Y.-T., Nicolella, D. P., Anderson, R. C., (1997). Probabilistic injury analysis of the cervical spine. AIAA-97-1135.

Toyota Central R&D LABS Inc., (2005). THUMS (Total HUman Model for Safety) Occupant Model: Version 2.21-040407.